Journal of Alloys and Compounds, 184 (1992) 175–185
JALCOM 179

Crystal and magnetic structure of the permanent magnetic material $Tm_2Fe_{14}C$

Ch. Hellwig and K. Girgis
Institut für Kristallographie und Petrographie, ETHZ, CH-8092 Zürich (Switzerland)

P. Fischer
Labor für Neutronenstreuung, ETHZ, CH-5232 Villigen PSI (Switzerland)

K. H. J. Buschow
Philips Research Laboratories, NL-5600 JA Eindhoven (Netherlands)

J. Schefer
Paul Scherrer Institut, CH-5232 Villigen PSI (Switzerland)

(Received November 17, 1991)

Abstract

$R_2Fe_{14}C$ (R, rare earth metal) compounds are considered as new permanent magnetic materials of technical interest. Investigations of the compound $Tm_2Fe_{14}C$ by means of X-ray and neutron diffraction as well as by metallographic techniques were carried out. $Tm_2Fe_{14}C$ crystallizes in the tetragonal space group $P4_2/mnm$ and is isotypic to $Nd_2Fe_{14}B$. The lattice constants are $a = 8.7304(2)$ Å and $c = 11.7640(4)$ Å at 295 K. The nuclear and magnetic structure of $Tm_2Fe_{14}C$ has been investigated by means of neutron diffraction at 650 K (above the Curie temperature T_C), 400 K (above the spin reorientation temperature T_{SR} and below T_C), room temperature and 10 K. The magnetic moments of all Tm and Fe atoms are always oriented collinear and antiparallel. Measurement of the magnetization curve by means of neutron diffraction yields a T_{SR} of 308 K, where the magnetization direction changes from parallel to the c axis above T_{SR} to perpendicular to the c axis below T_{SR}. The nuclear structure of $Tm_2Fe_{17}C_x$ (Th_2Ni_{17} structure type) has been refined simultaneously since this phase was also present in the sample.

1. Introduction

A promising group of permanent magnetic materials, $R_2Fe_{14}B$ (R = rare earth metal), was discovered in 1984 [1]. The magnetic and structural properties of these ternary compounds are reviewed in ref. 2. Substituting boron by carbon led to another promising group of permanent magnetic materials, the isotypic compounds $R_2Fe_{14}C$ [3–7]. Their Curie temperatures are slightly lower than those of the corresponding $R_2Fe_{14}B$ systems (*e.g.* 535 K for $Nd_2Fe_{14}C$ [8] compared with 585 K for $Nd_2Fe_{14}B$ [2]). However, the $R_2Fe_{14}C$ compounds have the advantage of the presence of a solid state transformation at high temperatures which can be used to obtain high coercivity bulk material without the necessity of employing the powder metallurgical

0925-8388/92/$5.00

route [2]. We have studied the magnetic structure of the compounds $Lu_2Fe_{14}C$, $Tb_2Fe_{14}C$ and $Ho_2Fe_{14}C$. All three compounds show a magnetization direction parallel to the c axis [9–11]. Different authors have studied the magnetic structure of $R_2Fe_{14}C$ for R ≡ Ce, Nd, Gd, Dy, Er and Lu [8, 12–16].

The aim of the present work is to study the magnetic structure of a compound with a predicted spin reorientation where the easy magnetization direction changes from perpendicular to the c axis below T_{SR} to parallel to the c axis above T_{SR}. The Curie temperature T_C is comparable with that of the $Lu_2Fe_{14}C$ compound. Bulk magnetization measurements showed that T_{SR} is 312 K [17] and that T_C is located between 495 and 500 K [7, 18].

2. Experimental details

The $Tm_2Fe_{14}C$ compound was prepared by arc melting from starting materials of at least 99.9% purity. Afterwards the sample was wrapped in tantalum foil and sealed in an evacuated quartz tube. Vacuum annealing was performed subsequently for 6 weeks at 900 °C. The microstructure of the annealed sample was studied by standard metallographic techniques. Microhardness measurements have been carried out to prove homogeneity.

X-ray powder photographs were obtained using a Guinier focusing camera (Jagodzinski type, Fe Kα radiation) with silicon as internal standard. The intensities were measured by means of an automatic Guinier film scanner.

Neutron diffraction measurements were carried out at high temperature (650 K) above T_C, between T_C and the spin reorientation temperature T_{SR} (400 K), at room temperature (295 K) and at low temperature (10 K). The measurements were performed on the multidetector powder diffractometer

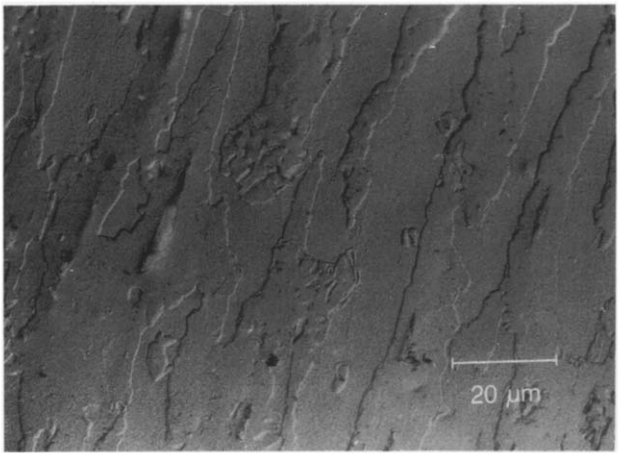

Fig. 1. Micrograph of $Tm_2Fe_{14}C$ sample. The sample was polished with diamond particles (size less than 1 μm) and subsequently electropolished in an ethanol–glycerin–HClO electrolyte. The two main phases are assumed to be $Tm_2Fe_{14}C$ and $Tm_2Fe_{17}C_x$ while the aggregations of small grains are assumed to be free iron.

TABLE 1

Change in the lattice constants of $Tm_2Fe_{14}C$ and $Tm_2Fe_{17}C_x$ with increasing temperature from 10 to 295 K and from 400 to 650 K determined by neutron diffraction measurements under identical experimental conditions

Temperature increase (K)	$Tm_2Fe_{14}C$		$Tm_2Fe_{17}C_x$	
	Δa (Å)	Δc (Å)	Δa (Å)	Δc (Å)
10–295	−0.0012(5)	0.016(1)	0.013(1)	−0.008(1)
400–650	−0.0078(4)	0.002(1)	0.004(2)	−0.003(1)

TABLE 2

Structural parameters of $Tm_2Fe_{14}C$ and $Tm_2Fe_{17}C_x$ at 650 K. The standard deviations of the lattice constants do not include errors from the neutron wavelength, $\Delta\lambda/\lambda$

Atom	Site	Parameter		
		x	y	z
Tm(1)	4f	0.2621(9)	0.2621(9)	0.000
Tm(2)	4g	0.1406(10)	0.8594(10)	0.000
Fe(1)	16k	0.2268(5)	0.5628(5)	0.1213(3)
Fe(2)	16k	0.0354(4)	0.3559(5)	0.1746(4)
Fe(3)	8j	0.0959(5)	0.0959(5)	0.2022(4)
Fe(4)	8j	0.3178(4)	0.3178(4)	0.2456(5)
Fe(5)	4e	0.000	0.000	0.6096(7)
Fe(6)	4c	0.000	0.500	0.000
C	4g	0.3675(11)	0.6325(11)	0.000
Results of refinement of second phase $Tm_2Fe_{17}C_x$				
Tm(1)	2b	0.000	0.000	0.250
Tm(2)	2d	0.333	0.667	0.750
Fe(1)	4f	0.333	0.667	0.107(1)
Fe(2)	6g	0.500	0.000	0.000
Fe(3)	12j	0.330(1)	0.956(1)	0.250
Fe(4)	12k	0.166(1)	0.332(1)	0.983(1)
C	6h	0.840(4)	0.681(8)	0.250
$B_{Tm}=0.99(10)$ Å^2		$B_{Fe}=0.72(1)$ Å^2		$B_C=2.09(24)$ Å^2
$Tm_2Fe_{14}C$:		$a,b=8.7224(3)$ Å		$c=11.7725(6)$ Å
$Tm_2Fe_{17}C_x$:		$a,b=8.527(1)$ Å		$c=8.345(1)$ Å
Occupation (C in $Tm_2Fe_{17}C_x$): 38(3)%				Others: 100%
$R_{nuclear}=5.8\%$		$R_{profile}=8.4\%$		$R_{expected}=4.6\%$

DMC [19] at the 10 MW reactor Saphir (PSI) with neutrons of wavelength $\lambda=1.701(2)$ and 1.706(2) Å. The magnetization curve was measured on the two-axis diffractometer at the reactor Saphir using neutrons of wavelength $\lambda=2.337(2)$ Å.

TABLE 3

Structural and magnetic parameters of $Tm_2Fe_{14}C$ and $Tm_2Fe_{17}C_x$ at 400 K (magnetic moments of $Tm_2Fe_{14}C$ are fixed parallel to the c axis, magnetic moments of $Tm_2Fe_{17}C_x$ perpendicular to the c axis). The standard deviations of the lattice constants do not include errors from the neutron wavelength, $\Delta\lambda/\lambda$

Atom	Site	Parameter			μ (μ_B)
		x	y	z	
Tm(1)	4f	0.2590(9)	0.2590(9)	0.000	0.3(2)
Tm(2)	4g	0.1404(9)	0.8596(9)	0.000	−0.1(2)
Fe(1)	16k	0.2252(4)	0.5632(4)	0.1214(3)	2.2(2)
Fe(2)	16k	0.0362(4)	0.3559(4)	0.1754(3)	2.1(2)
Fe(3)	8j	0.0953(4)	0.0953(4)	0.2033(4)	1.4(2)
Fe(4)	8j	0.3160(4)	0.3160(4)	0.2450(4)	2.9(2)
Fe(5)	4e	0.000	0.000	0.6101(6)	2.6(2)
Fe(6)	4c	0.000	0.500	0.000	2.2(3)
C	4g	0.3688(9)	0.6312(9)	0.000	0.0
Results of refinement of second phase $Tm_2Fe_{17}C_x$					
Tm(1)	2b	0.000	0.000	0.250	0.0
Tm(2)	2d	0.333	0.667	0.750	0.0
Fe(1)	4f	0.333	0.667	0.107(1)	2.5(2)
Fe(2)	6g	0.500	0.000	0.000	2.5(2)
F(3)	12j	0.329(1)	0.957(1)	0.250	2.5(2)
Fe(4)	12k	0.166(1)	0.332(1)	0.984(1)	2.5(2)
C	6h	0.845(3)	0.690(5)	0.250	0.0
$B_{Tm}=0.72(10)$ Å^2		$B_{Fe}=0.52(2)$ Å^2		$B_C=0.73(18)$ Å^2	
$Tm_2Fe_{14}C$:		$a,b=8.7302(3)$ Å		$c=11.7703(5)$ Å	
$Tm_2Fe_{17}C_x$:		$a,b=8.5223(8)$ Å		$c=8.3476(6)$ Å	
Occupation (C in $Tm_2Fe_{17}C_x$): 38%				Others: 100%	
$R_{nuclear}=4.7\%$		$R_{magnetic}=7.1\%$		$R_{profile}=7.1\%$	$R_{expected}=3.8\%$

3. Results

3.1. Metallographic differential thermal analysis (DTA) and X-ray results

Figure 1 shows a micrograph of the $Tm_2Fe_{14}C$ sample. Aggregations of small grains are visible in the matrix of the two main phases. These areas are assumed to be free iron whereas the two main phases are assumed to be $Tm_2Fe_{14}C$ and $Tm_2Fe_{17}C_x$. The microhardness measurements show that the sample is homogeneous. The distribution of the different phases is too fine (see micrograph of Fig. 1) to act as inhomogeneities for these measurements. The average value of 10 microhardness measurements amounts to 865(30) HV. DTA was performed at a heating rate of 10 K min^{-1}. It yields a single endothermic effect; therefore the values of T_C for $Tm_2Fe_{17}C_x$ and $Tm_2Fe_{14}C$ are assumed to be close together at 515 K. The X-ray data show that $Tm_2Fe_{14}C$ crystallizes in the tetragonal space group $P4_2/mnm$ (No. 136) with 68 atoms per unit cell and that the sample also contains a

TABLE 4

Structural and magnetic parameters of $Tm_2Fe_{14}C$ and $Tm_2Fe_{17}C_x$ at 295 K (all magnetic moments are fixed perpendicular to the c axis). The standard deviations of the lattice constants do not include errors from the neutron wavelength, $\Delta\lambda/\lambda$

Atom	Site	Parameter			μ (μ_B)
		x	y	z	
Tm(1)	4f	0.2624(10)	0.2624(10)	0.000	−2.9(2)
Tm(2)	4g	0.1409(10)	0.8591(10)	0.000	−2.7(2)
Fe(1)	16k	0.2267(5)	0.5638(5)	0.1201(4)	1.5(2)
Fe(2)	16k	0.0354(4)	0.3552(5)	0.1757(4)	1.9(1)
Fe(3)	8j	0.0963(5)	0.0963(5)	0.2030(4)	1.0(2)
Fe(4)	8j	0.3157(4)	0.3157(4)	0.2447(4)	2.0(1)
Fe(5)	4e	0.000	0.000	0.6098(7)	0.8(3)
Fe(6)	4c	0.000	0.500	0.000	1.6(2)
C	4g	0.3725(10)	0.6275(10)	0.000	0.0
Results of refinement of second phase $Tm_2Fe_{17}C_x$					
Tm(1)	2b	0.000	0.000	0.250	0.0
Tm(2)	2d	0.333	0.667	0.750	0.0
Fe(1)	4f	0.333	0.667	0.109(1)	2.9(3)
Fe(2)	6g	0.500	0.000	0.000	3.0(4)
Fe(3)	12j	0.329(1)	0.958(1)	0.250	2.7(2)
Fe(4)	12k	0.165(1)	0.331(1)	0.985(1)	3.4(2)
C	6h	0.846(3)	0.691(6)	0.250	0.0
$B_{Tm}=0.40(10)$ Å^2		$B_{Fe}=0.48(1)$ Å^2		$B_C=0.94(20)$ Å^2	
$Tm_2Fe_{14}C$:		$a,b=8.7351(3)$ Å		$c=11.7703(5)$ Å	
$Tm_2Fe_{17}C_x$:		$a,b=8.5223(8)$ Å		$c=8.3522(6)$ Å	
Occupation (C in $Tm_2Fe_{17}C_x$): 38%				Others: 100%	
$R_{nuclear}=6.0\%$		$R_{magnetic}=6.4\%$		$R_{profile}=7.8\%$	$R_{expected}=5.0\%$

certain amount of $Tm_2Fe_{17}C_x$. $Tm_2Fe_{17}C_x$ crystallizes in the hexagonal space group $P6_3/mmc$ (No. 194) with $38+2x$ atoms per unit cell. At room temperature the X-ray powder photographs yield lattice constants $a=8.7304(2)$ Å and $c=11.7640(4)$ Å for $Tm_2Fe_{14}C$ and $a=8.5181(8)$ Å and $c=8.3496(9)$ Å for $Tm_2Fe_{17}C_x$.

3.2. Nuclear and magnetic structure

We used as starting parameters those published in ref. 10 for $Tb_2Fe_{14}C$. The rare earth atoms are distributed over two point positions whereas the Fe atoms are distributed over six point positions; the C atoms occupy one further point position. As starting parameters for $Tm_2Fe_{17}C_x$ we used those found for the Th_2Ni_{17} type [20]. The rare earth atoms occupy two point positions whereas the Fe atoms are distributed over four point positions; the C atoms occupy the point position 6h according to ref. 21. We studied the sample at 650 K in the paramagnetic state without any magnetic influence on the structure refinement. The measurement at 400 K provides information about the magnetic structure between T_{SR} and T_C. The measurements at

TABLE 5

Structural and magnetic parameters of $Tm_2Fe_{14}C$ and $Tm_2Fe_{17}C_x$ at 10 K (magnetic moments of $Tm_2Fe_{14}C$ are fixed perpendicular to the c axis, magnetic moments of $Tm_2Fe_{17}C_x$ parallel to the c axis). The standard deviations of the lattice constants do not include errors from the neutron wavelength, $\Delta\lambda/\lambda$

Atom	Site	Parameter			μ (μ_B)
		x	y	z	
Tm(1)	4f	0.2582(12)	0.2582(12)	0.000	−5.4(1)
Tm(2)	4g	0.1381(11)	0.8619(11)	0.000	−6.1(2)
Fe(1)	16k	0.2274(6)	0.5636(6)	0.1225(5)	2.7(1)
Fe(2)	16k	0.0361(6)	0.3543(6)	0.1747(5)	3.5(1)
Fe(3)	8j	0.0960(6)	0.0960(6)	0.2048(6)	1.4(1)
Fe(4)	8j	0.3169(5)	0.3169(5)	0.2461(6)	2.9(1)
Fe(5)	4e	0.000	0.000	0.6083(9)	1.3(2)
Fe(6)	4c	0.000	0.500	0.000	3.8(2)
C	4g	0.3713(14)	0.6287(14)	0.000	0.0
Results of refinement of second phase $Tm_2Fe_{17}C_x$					
Tm(1)	2b	0.000	0.000	0.250	−5.4(5)
Tm(2)	2d	0.333	0.667	0.750	−8.0(3)
Fe(1)	4f	0.333	0.667	0.104(2)	1.7(3)
Fe(2)	6g	0.500	0.000	0.000	2.4(4)
Fe(3)	12j	0.331(2)	0.961(1)	0.250	1.9(2)
Fe(4)	12k	0.165(1)	0.331(2)	0.987(1)	2.6(3)
C	6h	0.848(4)	0.696(8)	0.250	0.0
$B_{Tm}=0.19(13)$ Å^2		$B_{Fe}=0.40(2)$ Å^2		$B_C=1.34(29)$ Å^2	
$Tm_2Fe_{14}C$:		$a,b=8.7363(4)$ Å		$c=11.7545(7)$ Å	
$Tm_2Fe_{17}C_x$:		$a,b=8.509(1)$ Å		$c=8.360(1)$ Å	
Occupation (C in $Tm_2Fe_{17}C_x$): 38%				Others: 100%	
$R_{nuclear}=5.0\%$		$R_{magnetic}=5.7\%$		$R_{profile}=8.0\%$	$R_{expected}=3.3\%$

room temperature and 10 K yield information about the magnetic structure below T_{SR}. The scattering lengths used for thulium, iron and carbon are 0.705×10^{-12}, 0.954×10^{-12} and 0.665×10^{-12} cm respectively [22]. The neutron magnetic form factors for Tm^{3+} and iron were taken from refs. 23 and 24 respectively. A three-phase Rietveld refinement was carried out owing to the presence of the $Tm_2Fe_{17}C_x$ phase and traces of free iron [25, 26]. For the determination of the occupation factor for carbon in the $Tm_2Fe_{17}C_x$ phase we used the 650 K data, since any magnetic influence is absent. The lattice constants change for $Tm_2Fe_{14}C$ and $Tm_2Fe_{17}C_x$ with increasing temperature. The changes in the temperature ranges 10–295 and 400–650 K were determined by neutron diffraction measurements under identical experimental conditions. The results are summarized in Table 1. All magnetic moments in both phases were refined collinear since this yields significantly better fits. The significantly best fits were achieved with the following directions of the magnetic moments: at 400 K the preferred direction is parallel to the c axis for $Tm_2Fe_{14}C$ and perpendicular to the c axis for $Tm_2Fe_{17}C_x$; at 295

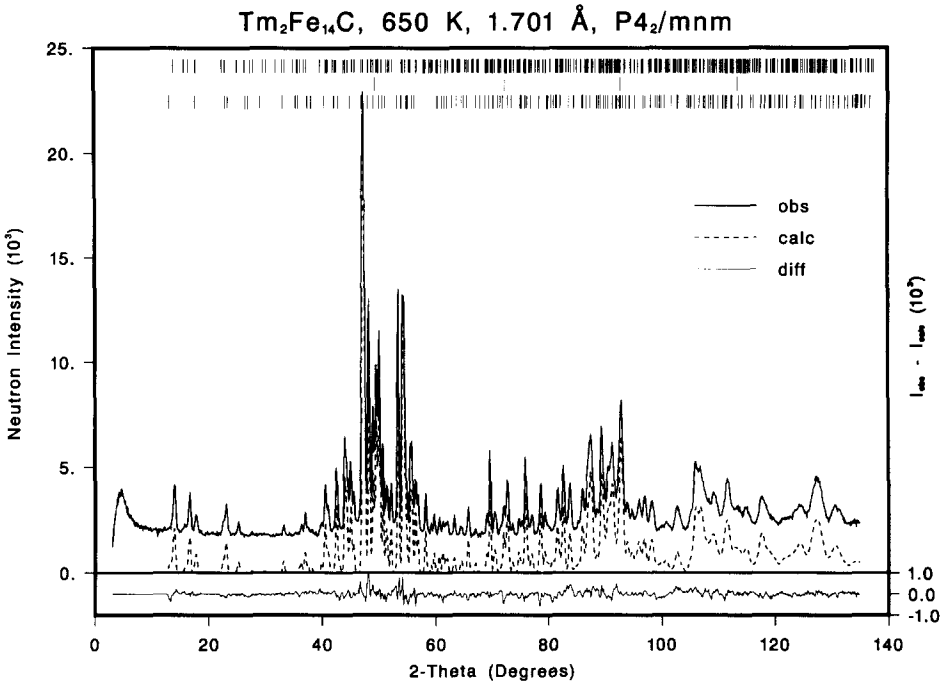

Fig. 2. Observed and calculated neutron diffraction patterns of paramagnetic $Tm_2Fe_{14}C$ at 650 K. The lines at the top indicate the positions of the following reflections: lower row, $Tm_2Fe_{17}C_x$; middle row, α-Fe; upper row, $Tm_2Fe_{14}C$.

K both phases have a preferred direction perpendicular to the c axis; at 10 K the preferred direction is perpendicular to the c axis for $Tm_2Fe_{14}C$ and parallel to the c axis for $Tm_2Fe_{17}C_x$. At 400 K the magnetic moments of thulium in $Tm_2Fe_{17}C_x$ were set to zero and the magnetic moments of iron in this phase were refined as a single value to achieve a better refinement. The results of the structure refinements are summarized in Tables 2–5 and three patterns are shown in Figs. 2–4. To obtain the magnetization curve of $Tm_2Fe_{14}C$, the temperature dependence of the integrated neutron intensity of the partial magnetic reflection (002) (magnetic intensity perpendicular to the c axis) and of the partial magnetic reflection (110) (magnetic intensity perpendicular to the 110 direction) was measured (Fig. 5). The magnetization M is proportional to $(I_{magn})^{1/2}$. T_{SR} was determined to be located at 308 K, but the location of T_C is not obvious from this graph since the decrease in the 110 reflection is very small at this temperature compared with the standard deviations.

4. Discussion

The compound $Tm_2Fe_{14}C$ crystallizes in the space group $P4_2/mnm$ (No. 136) similarly to $Nd_2Fe_{14}B$. The lattice constants at room temperature

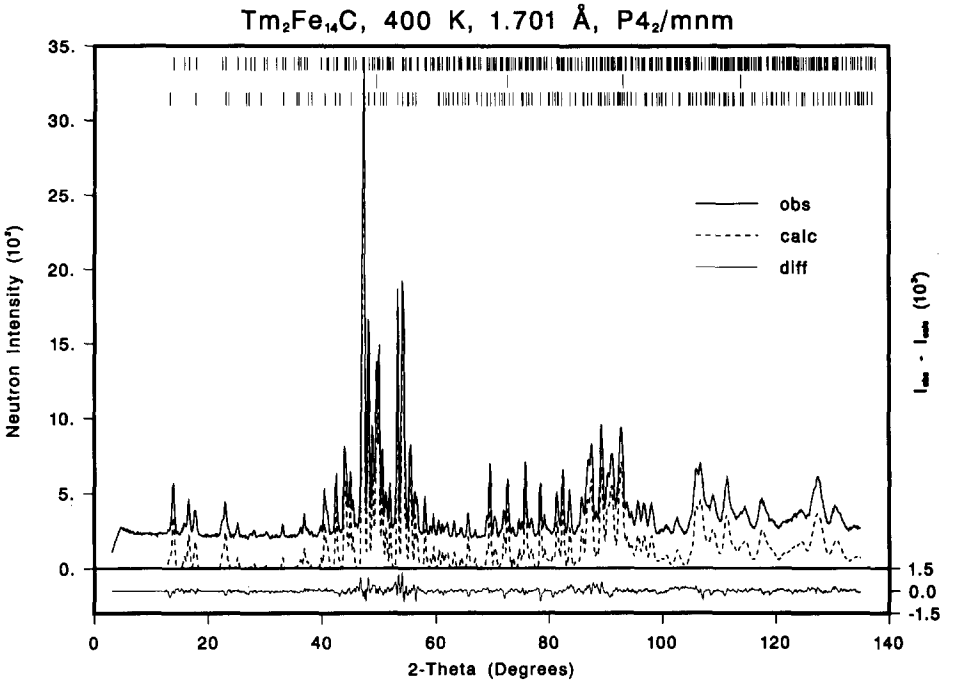

Fig. 3. Observed and calculated neutron diffraction patterns of ferromagnetic $Tm_2Fe_{14}C$ at 400 K. The lines at the top indicate the positions of the following reflections: lower row, $Tm_2Fe_{17}C_x$; middle row, α-Fe; upper row, $Tm_2Fe_{14}C$.

determined by X-ray diffraction are $a = 8.7304(2)$ Å and $c = 11.7640(4)$ Å. The lattice constant a decreases with increasing temperature whereas c increases.

For $Tm_2Fe_{14}C$ at 10 K all possible Schubnikow groups of $P4_2/mnm$ were tried without success [27]. Collinear magnetic moments perpendicular to the c axis yield the significantly best fit. No forbidden reflections were observed; therefore the n plane is preserved for the magnetic structure. We propose the Schubnikow space group $P2_1n'm'$ ($Pmn2_1$ is No. 31) for the magnetic structure of $Tm_2Fe_{14}C$ at 10 K with magnetic moments in the [100] direction (x', Schubnikow element). This is in agreement with results for $Tm_2Fe_{14}B$ [28]. The magnetic moments of $Tm_2Fe_{14}C$ at 400 K (above T_{SR} at 308 K) were refined parallel to the c axis since this yields a significantly better fit than refinement perpendicular to the c axis. The Schubnikow space group is $P4_2/mn'm'$ for this magnetic structure as it is for $R_2Fe_{14}C$ (R≡Tb, Dy, Ho, Lu) [9–11, 16]. The Tm atoms almost lose their magnetic moments; therefore the magnetic iron sublattice is similar to $Lu_2Fe_{14}C$ [9] where lutetium has no magnetic moment. The values of T_C are also comparable, showing the close relationship between these two structures. The Fe(4) atoms in the 8j position show the highest magnetic moment (2.9 μ_B) in the $Tm_2Fe_{14}C$ structure above T_{SR}. This is in good agreement with neutron diffraction measurements of $Nd_2Fe_{14}C$ [13], $Tb_2Fe_{14}C$ [10], $Dy_2Fe_{14}C$ [16], $Ho_2Fe_{14}C$

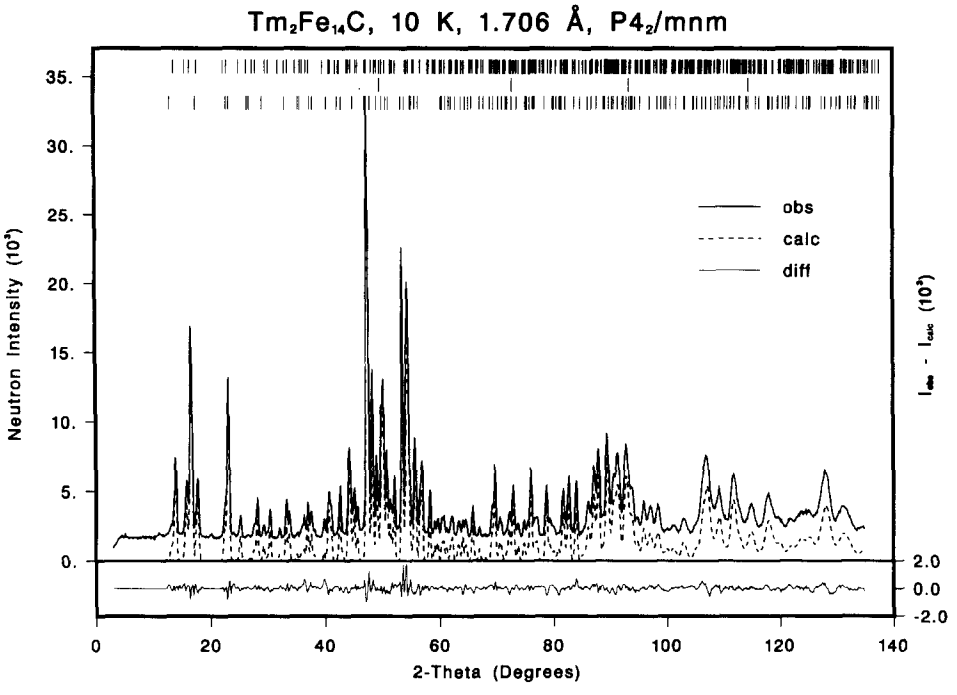

Fig. 4. Observed and calculated neutron diffraction patterns of ferromagnetic $Tm_2Fe_{14}C$ at 10 K. The lines at the top indicate the positions of the following reflections: lower row, $Tm_2Fe_{17}C_x$; middle row, α-Fe; upper row, $Tm_2Fe_{14}C$.

[11] and $Lu_2Fe_{14}C$ [9, 16]. The magnetic moments for Fe(4) atoms are the highest in all investigations on $Nd_2Fe_{14}B$-type compounds cited above.

The magnetic moments of the Fe atoms in $Tm_2Fe_{14}C$ below T_{SR} are not comparable with magnetic structures where $\mu \parallel c$. The Fe(2) and Fe(6) atoms in the 16k and 4c positions show the highest magnetic moments (3.5–3.8 μ_B), while the Fe(3) and Fe(5) atoms show the lowest magnetic moments (1.2–1.4 μ_B) in this structure. The saturation magnetization at 10 K is 27.0(5) μ_B f.u.$^{-1}$ (per formula unit), which is significantly higher than those determined by bulk magnetization measurements (16.8 [7] and 18.4 μ_B f.u.$^{-1}$ [17] respectively). This may be explained by the direct measurement by neutron diffraction in contrast to the bulk methods in the presence of other phases.

The $Tm_2Fe_{17}C_x$ phase changes its magnetization direction from parallel to the c axis at low temperatures to perpendicular to the c axis at higher temperatures. Comparing its T_C value with the values listed for various $Tm_2Fe_{17}C_x$ compounds in ref. 21, we expect its T_{SR} value to be close to 215 K. The present occupation factor for C_x yields $x = 1.1(1)$. This is in good agreement with the investigation cited above, where a T_C value of 498 K corresponds to $x = 1.0$. The Tm atoms almost lose their magnetic moments above T_{SR}, similarly to the $Tm_2Fe_{14}C$ phase. The magnetic determination of $Tm_2Fe_{17}C_x$ above T_{SR} presents the same problem as for $Tm_2Fe_{14}C$ below

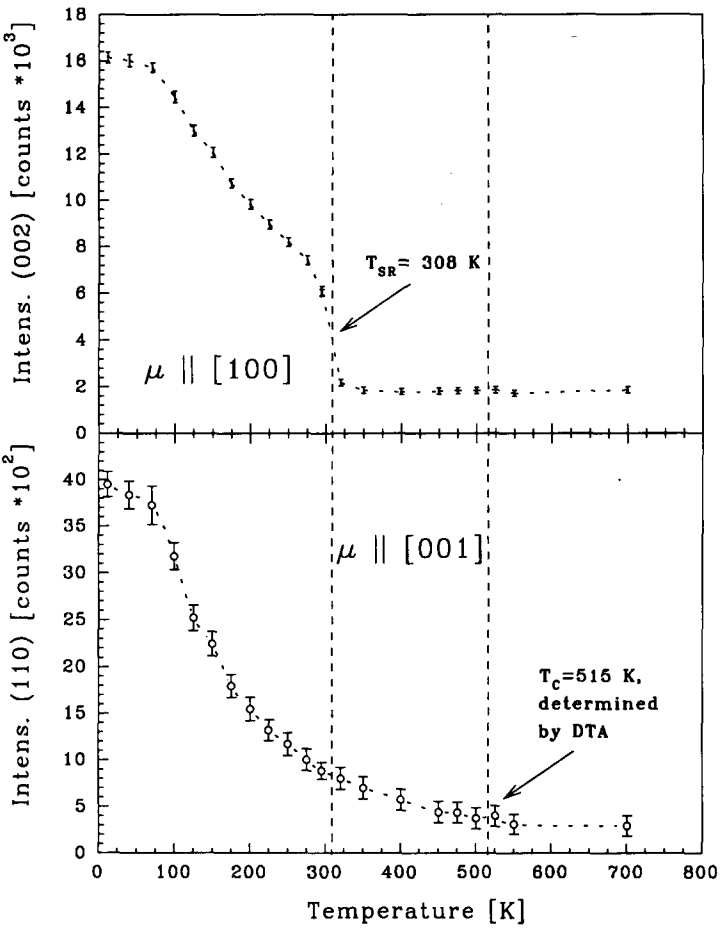

Fig. 5. Integrated neutron intensity of partial magnetic reflections (110) and (002) *vs.* temperature; $\lambda = 2.337(2)$ Å.

T_{SR}. No additional reflections were observed and all magnetic moments are collinear perpendicular to the c axis. Analogously to $Tm_2Fe_{14}C$ with $\mu \perp c$, we propose the Schubnikow space group $Cmc'm'$ and all magnetic moments to be along the [100] direction (*e.g.* equivalent to the [100] direction in the hexagonal lattice) or $Cm'cm'$ and all magnetic moments to be along the [010] direction (*e.g.* equivalent to the [120] direction in the hexagonal lattice).

Acknowledgments

We gratefully thank the workshop group of LNS (especially M. Koch) and the PSI reactor division for support and Professors W. M. Meier and P. Wachter for their interest. This work has been supported by the Swiss National Science Foundation.

References

1 M. Sagawa, S. Fujimura, M. Togawa and Y. Matsuura, *J. Appl. Phys.*, *55* (1984) 2083.
2 K. H. J. Buschow, in E. P. Wohlfarth and K. H. J. Buschow (eds.), *Ferromagnetic Materials*, Vol. 4, North-Holland, Amsterdam, 1988, p. 1.
3 E. P. Marusin, O. I. Bodak, A. O. Tsokol and V. S. Fundamenskii, *Sov. Phys. — Crystallogr.*, *30* (1985) 338.
4 C. Abache and H. Oesterreicher, *J. Appl. Phys.*, *57* (1985) 4112.
5 A. T. Pedziwiatr, W. E. Wallace and E. Burzo, *J. Magn. Magn. Mater.*, *59* (1986) L179.
6 N. C. Liu and H. H. Stadelmaier, *Mater. Lett.*, *4* (1986) 377.
7 M. Gueramian, A. Benzinge, K. Yvon and J. Müller, *Solid State Commun.*, *64* (1987) 639.
8 C. J. M. Denissen, B. D. de Mooij and K. H. J. Buschow, *J. Less-Common Met.*, *142* (1988) 195.
9 Ch. Hellwig, K. Girgis, J. Schefer, K. H. J. Buschow and P. Fischer, *J. Less-Common Met.*, *163* (1990) 361.
10 Ch. Helwig, K. Girgis, J. Schefer, K. H. J. Buschow and P. Fischer, *J. Less-Common Met.*, *169* (1991) 147.
11 Ch. Hellwig, K. Girgis, J. Schefer, K. H. J. Buschow and P. Fischer, *J. Alloys Comp 184* (1992) xxx.
12 T. H. Jacobs, C. J. M. Denissen and K. H. J. Buschow, *J. Less-Common Met.*, *153* (1989) L5.
13 R. B. Halmholdt and K. H. J. Buschow, *J. Less-Common Met.*, *144* (1988) L33.
14 K. H. J. Buschow, D. B. de Mooij and C. J. M. Denissen, *J. Less-Common Met.*, *141* (1988) L15.
15 K. Erdmann, T. Sinnemann, M. Rosenberg and K. H. J. Buschow, *J. Magn. Magn. Mater.*, *83* (1990) 130.
16 M. Yethiraj, W. B. Yelon and K. H. J. Buschow, *J. Magn. Magn. Mater.*, *97* (1991) 45.
17 R. Grössinger, R. Krewenka, X. C. Kou and K. H. J. Buschow, *J. Less-Common Met.*, *144* (1988) L33.
18 F. R. de Boer, Y.-K. Huang, Z.-D. Zhang, D. B. de Mooij and K. H. J. Buschow, *J. Magn. Magn. Mater.*, *72* (1988) 167.
19 J. Schefer, P. Fischer, H. Heer, A. Isacson, M. Koch and R. Thut, *Nucl. Instrum. Methods A*, *288* (1990) 477.
20 W. B. Pearson, *Handbook of Lattice Spacings and Structures of Metals*, Vol. 2, Pergamon, Oxford, 1967, p. 399.
21 P. C. M. Gubbens, A. M. van der Kraan, T. H. Jacobs and K. H. J. Buschow, *J. Magn. Magn. Mater.*, *80* (1989) 265.
22 V. F. Sears, *Methods Exp. Phys. A*, *23* (1986) 521.
23 A. J. Freeman and J. P. Desclaux, *J. Magn. Magn. Mater.*, *12* (1979) 11–21.
24 R. M. Moon, *Int. J. Magn.*, *1* (1971) 219.
25 H. M. Rietveld, *J. Appl. Crystallogr.*, *2* (1969) 65.
26 A. W. Hewat, *Harwell Rep. AERE-R7350*, 1973.
27 W. Opechowski and R. Guccione, in G. T. Rado and H. Suhl (eds.), *Magnetism*, Vol. 2a, Academic, New York, 1965, p. 105.
28 S. Hirosawa and M. Sagawa, *Solid State Commun.*, *54* (1985) 335.